

Supplemental Methods

Phylogenetic analysis

Multiple sequence alignments were created using the ClustalW Sequence Alignment program of the Molecular Evolution Genetics Analysis software 6 (MEGA6).¹

Phylogenetic trees for the three datasets were constructed using the distance-based neighbor-joining (NJ) method using MEGA6, and phylogenetic trees for the exon 2 dataset were additionally constructed using the model-based maximum likelihood (ML) and Bayesian inference (BI) methods. The NJ trees were constructed using distances corrected according to the maximum composite likelihood model with 1.0 gamma parameters and assessed using 1,000 bootstrap replicates. For the ML analyses we used MrAIC Ver. 1.4.4² with PhyML Ver. 3.0³ to estimate the most likely model of the sequence evolution. Based on maximum likelihood values and the corrected Akaike information criterion (AICc), the HKY+I model was selected as the most likely model ($-\ln l = -594.7825$, $AIC = 1284.2734$) for nucleotide-based ML trees. Phylogenetic trees were constructed by the MEGA6 with the HKY+I model and assessed using 1,000 bootstrap replicates. For the BI analyses, we used MrAIC Ver. 1.4.4 with PhyML Ver. 3.0 to estimate the most likely model of sequence evolution. Based on maximum likelihood values and the Bayesian information criterion (BIC), the F81+I model was selected as the most likely model ($-\ln l = -597.3650$, $BIC = 1412.1921$) for the BI method. Phylogenetic trees were constructed by the character-based BI method (MrBayes Ver. 3.1.2)⁴. The Bayesian analysis was run using the Metropolis coupled Markov Chain Monte Carlo (MCMC) algorithm from randomly generated starting trees for 1,000,000 generations, with sampling every 100 generations. The first 100,100 steps of each run were discarded as burn in. Convergence for both runs was examined using the average standard deviation of the split frequencies and through examination of the Markov Chain Monte Carlo chains using Tracer v1.6

(<http://beast.bio.ed.ac.uk/Tracer>).⁵

References

1. Tamura K, Stecher G, Peterson D, Filipski A, Kumar S. MEGA6: Molecular Evolutionary Genetics Analysis version 6.0. *Mol Biol Evol.* 2013;30(12):2725-2729.
2. Nylander J. 2004; Available at: <http://www.abc.se/~nylander/>.
3. Guindon S, Dufayard JF, Lefort V, Anisimova M, Hordijk W, Gascuel O. New algorithms and methods to estimate maximum-likelihood phylogenies: assessing the performance of PhyML 3.0. *Syst Biol.* 2010;59(3):307-321.
4. Ronquist F, Huelsenbeck JP. MrBayes 3: Bayesian phylogenetic inference under mixed models. *Bioinformatics.* 2003;19(12):1572-1574.
5. Rambaut A, Suchard MA, Xie D, Drummond AJ. 2014; Tracer v1.6, Available from <http://beast.bio.ed.ac.uk/Tracer>.

Supplemental Table S1: Effect of HLA-DPB1 T-cell epitope mismatching on transplant outcomes

Clinical outcome	HLA-DPB1 TCE mismatch	HR	(95% CI)	P
aGVHD II-IV	Permissive	1.00		
	non-permissive	1.24	(1.02-1.49)	0.028
aGVHD III-IV	Permissive	1.00		
	non-permissive	1.37	(1.00-1.86)	0.047
Relapse	Permissive	1.00		
	non-permissive	0.89	(0.68-1.17)	0.424
Transplant-related mortality	Permissive	1.00		
	non-permissive	1.16	(0.89-1.50)	0.905
Overall mortality	Permissive	1.00		
	non-permissive	1.15	(0.95-1.39)	0.877

TCE: T-cell epitope; HR: hazard ratio indicates comparison of the TCE non-permissive mismatch to the permissive mismatch; CI: confidence interval.

Number of patients: Permissive (n=954), Non-permissive (n=332).

Supplemental Table S2: Relation of difference in functional distance scores of HLA-DPB1 to TCE mismatching and patient mismatch HLA-DP group

Difference in functional distance scores of HLA-DPB1					
		D-FD≤2.665 (N=1077)		D-FD>2.665 (N=209)	
P value					
HLA-DPB1 TCE mismatching, no. (%)					
Permissive	930	(86.4)	24	(11.4)	<0.001
Non-permissive	147	(13.6)	185	(88.5)	
Patient mismatch HLA-DP group, no. (%)					
HLA-DP2 group	585	(54.3)	72	(34.4)	<0.001
HLA-DP5 group	492	(45.7)	137	(65.6)	

The difference in functional distance scores of patient and donor HLA-DPB1 alleles was defined according to a previously published algorithm.^{1,2}

N: number of patients; D-FD: difference in functional distance scores of patient and donor HLA-DPB1 alleles; TCE: T-cell epitope.

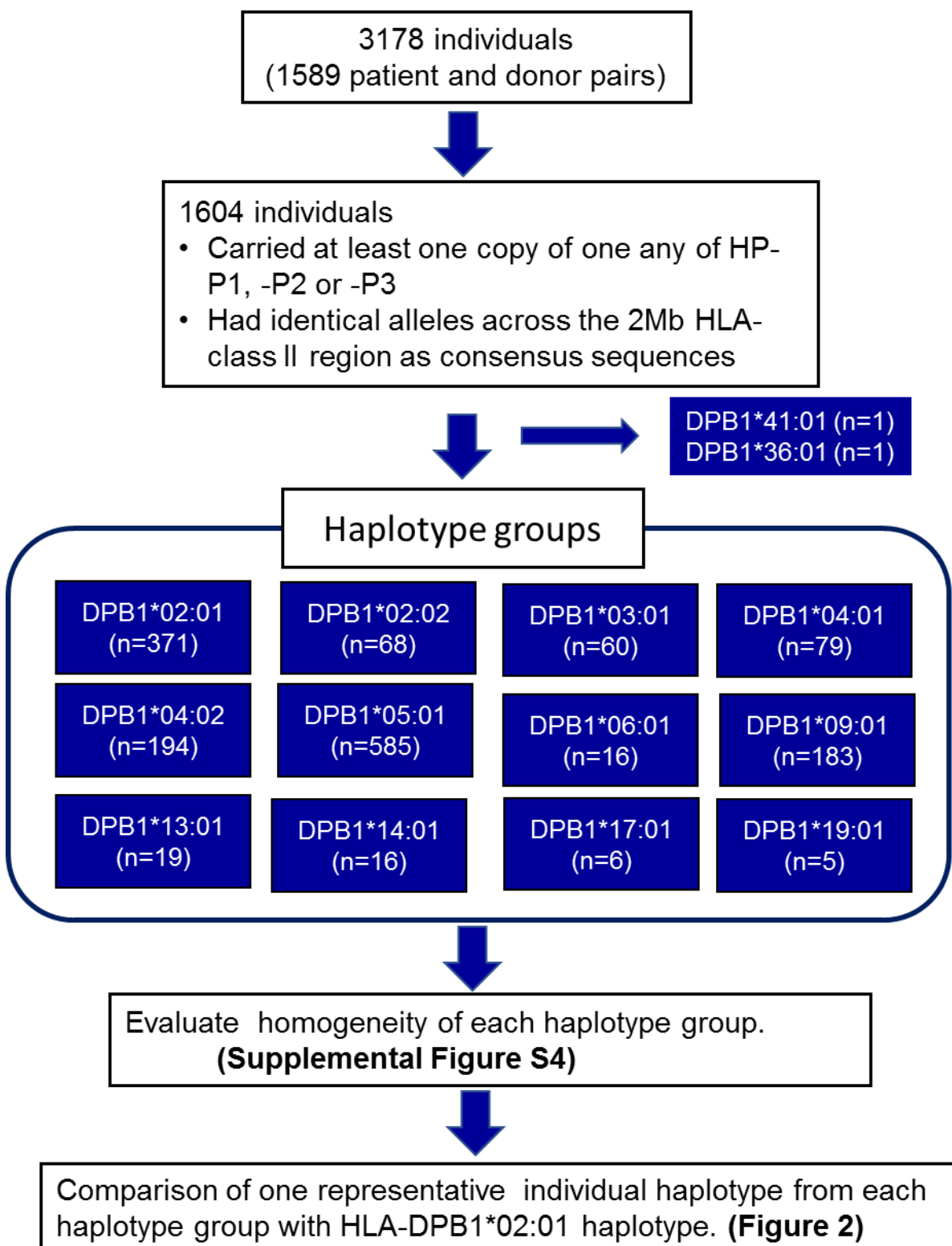
References

1. Crivello P, Zito L, Sizzano F, et al. The impact of amino acid variability on alloreactivity defines a functional distance predictive of permissive HLA-DPB1 mismatches in hematopoietic stem cell transplantation. *Biol Blood Marrow Transplant.* 2015;21(2):233-241.
2. Crivello P, Heinold A, Rebmann V, et al. Functional distance between recipient and donor HLA-DPB1 determines nonpermissive mismatches in unrelated HCT. *Blood.* 2016;128(1):120-129.

Supplemental Table S3: Association of patient mismatch HLA-DP group and the difference in functional distance scores of patient and donor HLA-DPB1 alleles

		HR	(95% CI)	P	N
Patient mismatch HLA-DP group effect					
D-FD \leq 2.665	DP2 group	1.00			585
	DP5 group	1.39	(1.15-1.68)	0.001	492
D-FD $>$ 2.665	DP2 group	1.00			72
	DP5 group	0.74	(0.46-1.10)	0.129	137
D-FD effect			(95% CI)	P	N
DP2 group	D-FD \leq 2.665	1.00			585
	D-FD $>$ 2.665	1.83	(1.32-2.62)	0.001	72
DP5 group	D-FD \leq 2.665	1.00			492
	D-FD $>$ 2.665	0.97	(0.73-1.30)	0.851	137

N: number of patients; D-FD: the difference in functional distance scores of patient and donor HLA-DPB1 alleles; HR: hazard ratio indicates comparison of the D-FD \leq 2.665 to the D-FD $>$ 2.665; CI: confidence interval; N: number of patients.

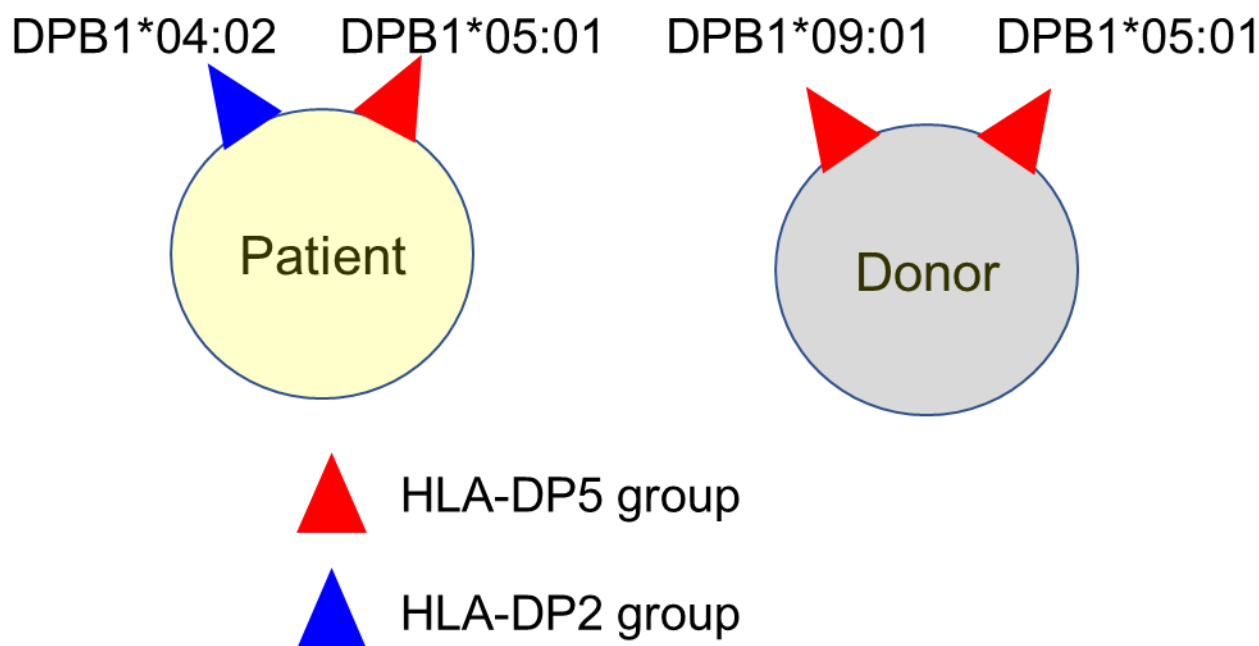


Supplemental Figure S1

Supplemental Figure S1: Schematic diagram of Multi-SNP analysis of HLA-DPB1 haplotypes

Multi-SNP data in HLA region of 3178 individuals (1589 patient and donor pairs) performed genome-wide association studies were analyzed in this study. Among them, 1604 individuals carried at least one copy of any of HP-P1 (HLA-A*24:02 -Cw*12:02 -B*52:01 -DRB1*15:02 -DQB1*06:01 -DPB1*09:01), -P2 (HLA-A*3303 -Cw*14:03 -B*44:03 -DRB1*13:02 -DQB1*06:04 -DPB1*04:01) or -P3 (HLA-A*24:02 -Cw*07:02 -B*07:02 -DRB1*01:01 -DQB1*05:01 -DPB1*04:02), and had identical alleles for more than 99.5% of 3246 consecutive SNPs across the 2 Mb HLA-class II region as consensus sequences of these haplotypes.

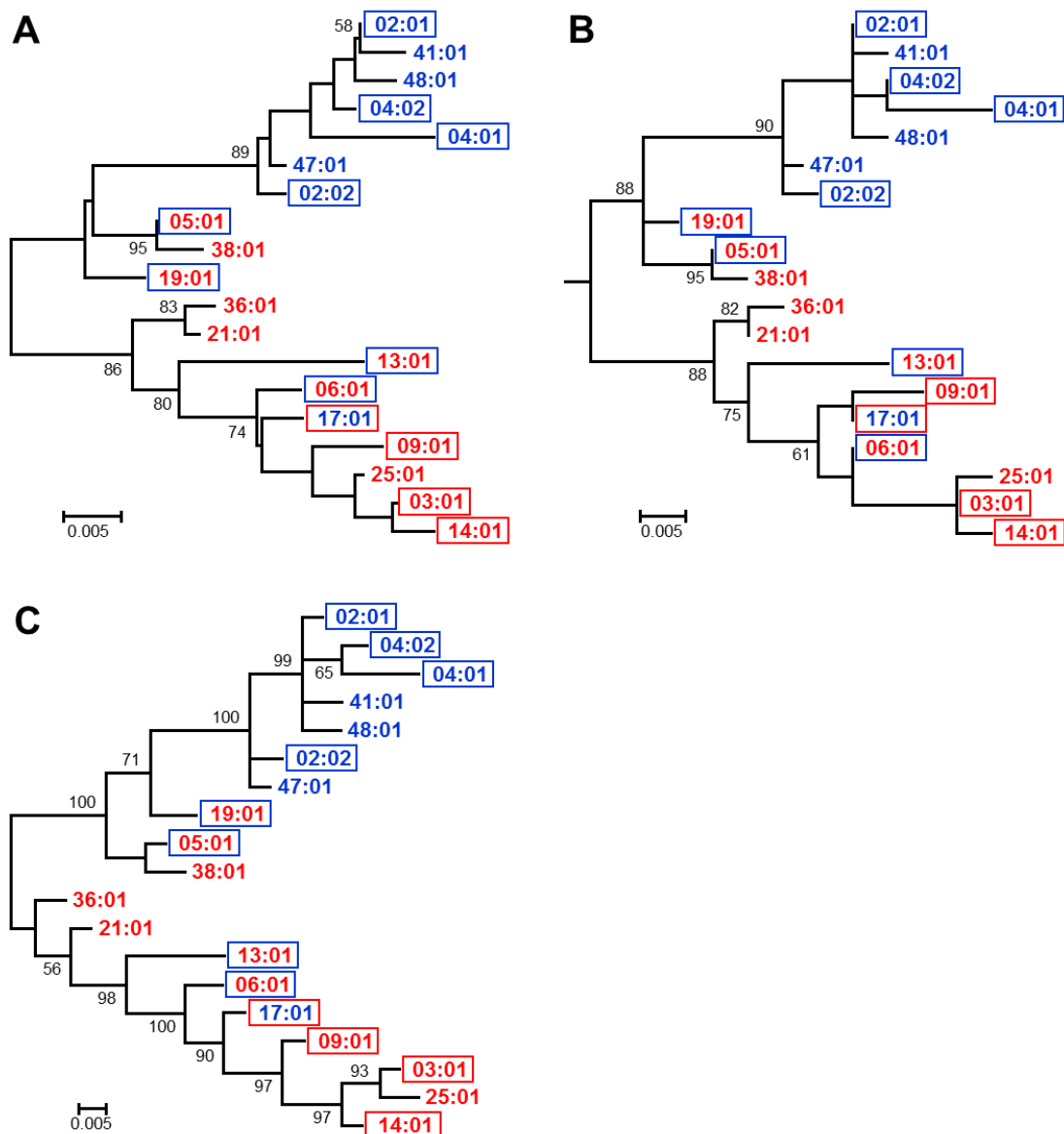
There were 12 HLA-DPB1 haplotype groups with more than 5 individual haplotypes. We confirmed the homogeneity of each HLA-DPB1 haplotype group, and one representative individual haplotype from each haplotype group was compared with the HLA-DPB1*02:01 haplotype for comparison between haplotype groups.



Supplemental Figure S2

Supplemental Figure S2: Association between patient and donor mismatch HLA-DP groups

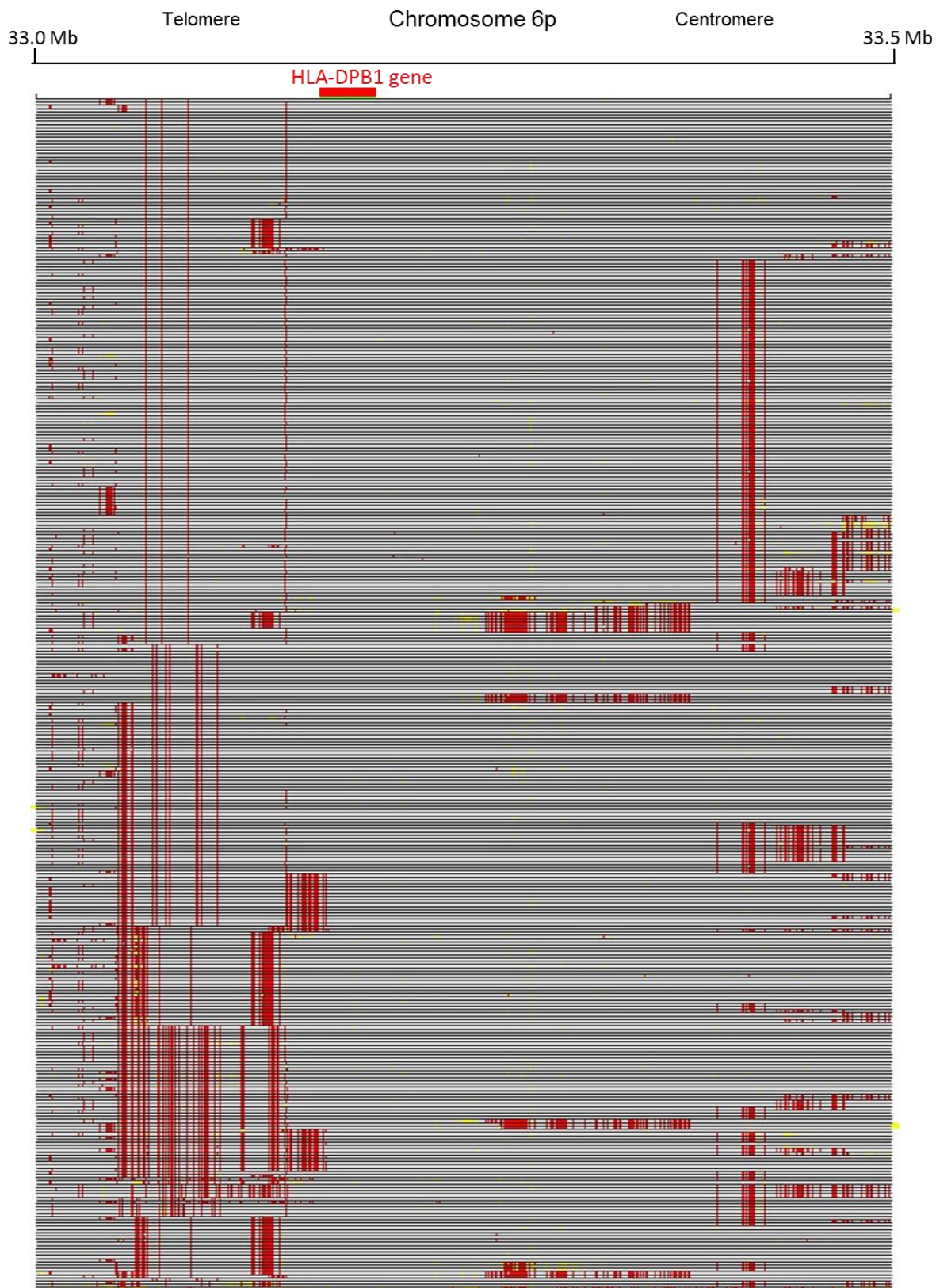
Transplant outcomes were assessed in 1286 patients transplanted from donors who were HLA-A-, -B-, -C-, -DRB1-, and -DQB1-matched and had only one HLA-DPB1 mismatch in the GVH direction. In this example, patient mismatch HLA-DPB1 is HLA-DPB1*04:02, therefore patient mismatch HLA-DP group is HLA-DP2 group. On the other hand, donor mismatch HLA-DPB1 is HLA-DPB1*09:01, therefore donor mismatch HLA-DP group is HLA-DP5 group.



Supplemental Figure S3

Supplemental Figure S3: Neighbor joining (A), maximum likelihood (B) and Bayesian inference (C) phylogenies depicting genetic relationships among 19 representative HLA-DPB1 allele sequences.

The 264 bp nucleotide alignment was used for the analysis. Numbers shown on the branches are bootstrap support values in A and B and posterior probability in C. Blue and red letters indicate DP2 group (rs9277534: A) and DP5 group (rs9277534: G) alleles, respectively. Blue and red frames indicate predicted immunogenicity groups, “Group 3” and “Group 1 or 2” defined by Zino et al. (2004), respectively.



Supplemental Figure S4

Supplemental Figure S4: Homogeneity of HLA-DPB1*02:01 haplotype.

HLA-DPB1*02:01 haplotypes from each of 369 individuals were compared with consensus SNP sequence across the 0.5 Mb region. Each row indicates one haplotype. Gray SNPs are identical to the consensus alleles, while red SNPs are different from the consensus alleles. Yellow markers indicate missing SNPs.